STRESS-STRAIN CURVE OF FCC INTERSTITIAL ALLOY AuSi UNDER PRESSURE

N. Q. HỌC[1], B. D. TINH[1], N. D. HIEN[2]

[1] Hanoi National University of Education, 136 Xuan Thuy, Cau Giay, Hanoi, Vietnam
E-mail: hocnq@hnue.edu.vn
Corresponding author e-mail: tinhbd@hnue.edu.vn
[2] Mac Dinh Chi High School, Chu Pah district, Gia Lai province

Received April 10, 2020

Abstract. Analytic expressions of characteristic nonlinear deformation quantities such as the density of deformation energy, the maximum real stress and the limit of elastic deformation for FCC interstitial alloy AB under pressure are derived from the statistical moment method. The theoretical results are applied numerically to AuSi and the calculated results are compared with ones of Au and experiments.

Key words: interstitial alloy, nonlinear deformation, density of deformation energy, maximum real stress, limit of elastic deformation and statistical moment method.

1. INTRODUCTION

Elastic and thermodynamic properties of interstitial alloys have been interested by theoretical and experimental researchers [1–19]. Examples are the theory of interstitial alloy [2, 3], calculations from first principles, many-body potentials and dynamical dynamics for defects in metals, alloys and solid solutions [4–6], elastic and thermodynamic properties of perfect ternary and binary interstitial alloys [9–19]. We have been studied the elastic deformation for *body-centered cubic* (BCC) and *face-centered cubic* (FCC) ternary and binary interstitial alloys under pressure in [9–18] and the theory of nonlinear deformation for BCC and FCC ternary interstitial alloys under pressure in [19] by the *statistical moment method* (SMM).

The dependence of elastic and nonlinear deformations of materials on temperature and pressure has very important role in predicting and understanding their interatomic interactions, strength, mechanical stability, phase transition mechanisms and dynamical response. Silicides such as iron silicides have attracted a lot of attention in recent years because of their functional applications and unusual physical properties. For example the β-$FeSi_2$ is a material for thermoelectric conversion, solar cells and optoelectronic applications. Gold silicide or gold silicon is one of numerous metal alloys with the trade name AE Alloys^{TM}. These alloys are available as ingot, ribbon, bar, shot, wire, foil and sheet. Ultra-high-purity and

high-purity forms also include metal powder, micron powder, nanoscale, pellets for *chemical vapor deposition* (CVD) and targets for thin film deposition and *physical vapor deposition* (PVD) applications. Custom and typical packaging is available. Primary applications include bearing assembly, casting, ballast, radiation shielding and step soldering.

In present paper, we will study nonlinear deformations of FCC binary interstitial alloy under pressure. In Section 2, we build the model and theoretical calculations and in Section 3, we carry out numerical calculations for alloy AuSi.

2. MODEL AND THEORETICAL CALCULATIONS

In the interstitial alloy AB with FCC structure, the cohesive energy u_0 and the alloy parameters k, γ_1, γ_2, γ for the interstitial atom B (which stays in body center of cubic unit cell), the main metal atom A_1 (which stays in face center of cubic unit cell) and the main metal atom A_2 (which stays in peaks of cubic unit cell) in the approximation of two coordination spheres have the form [9–20]

$$u_{0B} = \frac{1}{2}\sum_{i=1}^{n_i}\varphi_{AB}(r_i) = 3\varphi_{AB}\left(r_{1B}\right) + 4\varphi_{AB}\left(r_{2B}\right), \quad r_{2B} = \sqrt{3}r_{1B},$$

$$k_B = \frac{1}{2}\sum_i\left(\frac{\partial^2\varphi_{AB}}{\partial u_{i\beta}^2}\right)_{eq} = \frac{d^2\varphi_{AB}\left(r_{1B}\right)}{dr_{1B}^2} + \frac{2}{r_{1B}}\frac{d\varphi_{AB}\left(r_{1B}\right)}{dr_{1B}} +$$
$$+\frac{4}{3}\frac{d^2\varphi_{AB}\left(r_{2B}\right)}{dr_{2B}^2} + \frac{8}{3r_{2B}}\frac{d\varphi_{AB}\left(r_{2B}\right)}{dr_{2B}}, \gamma_B = 4\left(\gamma_{1B} + \gamma_{2B}\right),$$

$$\gamma_{1B} = \frac{1}{48}\sum_i\left(\frac{\partial^4\varphi_{AB}}{\partial u_{i\beta}^4}\right)_{eq} = \frac{1}{24}\frac{d^4\varphi_{AB}(r_{1B})}{dr_{1B}^4} + \frac{1}{4r_{1B}^2}\frac{d^2\varphi_{AB}(r_{1B})}{dr_{1B}^2} - \frac{1}{4r_{1B}^3}\frac{d\varphi_{AB}(r_{1B})}{dr_{1B}} +$$
$$+\frac{1}{54}\frac{d^4\varphi_{AB}(r_{2B})}{dr_{2B}^4} + \frac{2}{9r_{2B}}\frac{d^3\varphi_{AB}(r_{2B})}{dr_{2B}^3} - \frac{2}{9r_{2B}^2}\frac{d^2\varphi_{AB}(r_{2B})}{dr_{2B}^2} + \frac{2}{9r_{2B}^3}\frac{d\varphi_{AB}(r_{2B})}{dr_{2B}},$$

$$\gamma_{2B} = \frac{6}{48}\sum_i\left(\frac{\partial^4\varphi_{AB}}{\partial u_{i\alpha}^2\partial u_{i\beta}^2}\right)_{eq} = \frac{1}{2r_{1B}}\frac{d^3\varphi_{AB}(r_{1B})}{dr_{1B}^3} - \frac{3}{4r_{1B}^2}\frac{d^2\varphi_{AB}(r_{1B})}{dr_{1B}^2} + \frac{3}{4r_{1B}^3}\frac{d\varphi_{AB}(r_{1B})}{dr_{1B}} +$$
$$+\frac{1}{9}\frac{d^4\varphi_{AB}(r_{2B})}{dr_{2B}^4} + \frac{2}{3r_{2B}^2}\frac{d^2\varphi_{AB}(r_{2B})}{dr_{2B}^2} - \frac{2}{3r_{2B}^3}\frac{d\varphi_{AB}(r_{2B})}{dr_{2B}}, u_{0A_1} = u_{0A} + \varphi_{AB}\left(r_{1A_1}\right),$$

$$k_{A_1} = k_A + \frac{1}{2}\sum_i \left[\left(\frac{\partial^2 \varphi_{AB}}{\partial u_{i\beta}^2}\right)_{eq}\right]_{r=r_{1A_1}} = k_A + \frac{d^2\varphi_{AB}\left(r_{1A_1}\right)}{dr_{1A_1}^2}, \gamma_{A_1} = 4\left(\gamma_{1A_1} + \gamma_{2A_1}\right),$$

$$\gamma_{1A_1} = \gamma_{1A} + \frac{1}{48}\sum_i \left[\left(\frac{\partial^4 \varphi_{AB}}{\partial u_{i\beta}^4}\right)_{eq}\right]_{r=r_{1A_1}} = \gamma_{1A} + \frac{1}{24}\frac{d^4\varphi_{AB}(r_{1A_1})}{dr_{1A_1}^4},$$

$$\gamma_{2A_1} = \gamma_{2A} + \frac{6}{48}\sum_i \left[\left(\frac{\partial^4 \varphi_{AB}}{\partial u_{i\alpha}^2 \partial u_{i\beta}^2}\right)_{eq}\right]_{r=r_{1A_1}} = \gamma_{2A} + \frac{1}{4r_{1A_1}}\frac{d^3\varphi_{AB}(r_{1A_1})}{dr_{1A_1}^3} -$$

$$-\frac{1}{2r_{1A_1}^2}\frac{d^2\varphi_{AB}(r_{1A_1})}{dr_{1A_1}^2} + \frac{1}{2r_{1A_1}^3}\frac{d\varphi_{AB}(r_{1A_1})}{dr_{1A_1}}, u_{0A_2} = u_{0A} + \varphi_{AB}\left(r_{1A_2}\right),$$

$$k_{A_2} = k_A + \frac{1}{2}\sum_i \left[\left(\frac{\partial^2 \varphi_{AB}}{\partial u_{i\beta}^2}\right)_{eq}\right]_{r=r_{1A_2}} = k_A + \frac{1}{6}\frac{d^2\varphi_{AB}\left(r_{1A_2}\right)}{dr_{1A_2}^2} + \frac{23}{6r_{1A_2}}\frac{d\varphi_{AB}\left(r_{1A_2}\right)}{dr_{1A_2}},$$

$$\gamma_{A_2} = 4\left(\gamma_{1A_2} + \gamma_{2A_2}\right), \gamma_{1A_2} = \gamma_{1A} + \frac{1}{48}\sum_i \left[\left(\frac{\partial^4 j_{AB}}{\partial u_{i\beta}^4}\right)_{eq}\right]_{r=r_{1A_2}} = \gamma_{1A} +$$

$$+\frac{1}{54}\frac{d^4\varphi_{AB}(r_{1A_2})}{dr_{1A_2}^4} + \frac{2}{9r_{1A_2}}\frac{d^3\varphi_{AB}(r_{1A_2})}{dr_{1A_2}^3} - \frac{2}{9r_{1A_2}^2}\frac{d^2\varphi_{AB}(r_{1A_2})}{dr_{1A_2}^2} + \frac{2}{9r_{1A_2}^3}\frac{d\varphi_{AB}(r_{1A_2})}{dr_{1A_2}},$$

$$\gamma_{2A_2} = \gamma_{2A} + \frac{6}{48}\sum_i \left[\left(\frac{\partial^4 \varphi_{AB}}{\partial u_{i\alpha}^2 \partial u_{i\beta}^2}\right)_{eq}\right]_{r=r_{1A_2}} = \gamma_{2A} + \frac{1}{81}\frac{d^4\varphi_{AB}(r_{1A_2})}{dr_{1A_2}^4} + \quad (1)$$

$$+\frac{4}{27r_{1A_2}}\frac{d^3\varphi_{AB}(r_{1A_2})}{dr_{1A_2}^3} + \frac{14}{27r_{1A_2}^2}\frac{d^2\varphi_{AB}(r_{1A_2})}{dr_{1A_2}^2} - \frac{14}{27r_{1A_2}^3}\frac{d\varphi_{AB}(r_{1A_2})}{dr_{1A_2}},$$

where φ_{AB} is the interaction potential between atoms A and B, $r_{1X} = r_{0X} + y_{0X}(T)$ is the nearest neighbor distance between the atom X (X = A, A_1, A_2, B) (A in clean metal, A_1, A_2 and B in interstitial alloy AB) and other atom at temperature T, r_{01X} is the nearest neighbor distance between the atom X and other atom at T = 0K and is determined from the minimum condition of the cohesive energy u_{0X}, $y_{0X}(T)$ is the

displacement of atom X from equilibrium position at temperature T, u_{0A}, k_A, γ_{1A}, γ_{2A}, γ_A are the corresponding quantities in the clean metal A with FCC structure in the approximation of two coordination spheres [20]

$$u_{0A} = 6\varphi_{AA}(r_{1A}) + 3\varphi_{AA}(r_{2A}), \quad r_{2A} = \sqrt{2}r_{1A},$$

$$k_A = 2\frac{d^2\varphi_{AA}(r_{1A})}{dr_{1A}^2} + \frac{4}{r_{1A}}\frac{d\varphi_{AA}(r_{1A})}{dr_{1A}} + \frac{d^2\varphi_{AA}(r_{2A})}{dr_{2A}^2} + \frac{2}{r_{2A}}\frac{d\varphi_{AA}(r_{2A})}{dr_{2A}},$$

$$\gamma_{1A} = \frac{1}{24}\frac{d^4\varphi_{AA}(r_{1A})}{dr_{1A}^4} + \frac{1}{4r_{1A}}\frac{d^3\varphi_{AA}(r_{1A})}{dr_{1A}^3} - \frac{1}{8r_{1A}^2}\frac{d^2\varphi_{AA}(r_{1A})}{dr_{1A}^2} + \frac{1}{8r_{1A}^3}\frac{d\varphi_{AA}(r_{1A})}{dr_{1A}} + \frac{1}{24}\frac{d^4\varphi_{AA}(r_{2A})}{dr_{2A}^4} + \frac{1}{4r_{2A}^2}\frac{d^2\varphi_{AA}(r_{2A})}{dr_{2A}^2} - \frac{1}{4r_{2A}^3}\frac{d\varphi_{AA}(r_{2A})}{dr_{2A}},$$

$$\gamma_{2A} = \frac{1}{48}\frac{d^4\varphi_{AA}(r_{1A})}{dr_{1A}^4} + \frac{7}{8r_{1A}}\frac{d^3\varphi_{AA}(r_{1A})}{dr_{1A}^3} - \frac{31}{16r_{1A}^2}\frac{d^2\varphi_{AA}(r_{1A})}{dr_{1A}^2} + \frac{31}{16r_{1A}^3}\frac{d\varphi_{AA}(r_{1A})}{dr_{1A}} + \frac{1}{2r_{2A}}\frac{d^3\varphi_{AA}(r_{2A})}{dr_{2A}^3} - \frac{9}{8r_{2A}^2}\frac{d^2\varphi_{AA}(r_{2A})}{dr_{2A}^2} + \frac{9}{8r_{2A}^3}\frac{d\varphi_{AA}(r_{2A})}{dr_{2A}}, \quad \gamma_A = 4(\gamma_{1A} + \gamma_{2A}) \tag{2}$$

The equation of state for FCC interstitial alloy at temperature T and pressure P is written in the form [9, 16, 20]

$$Pv = -r_l\left(\frac{1}{6}\frac{\partial u_0}{\partial r_l} + \theta x\,\mathrm{cth}x\,\frac{1}{2k}\frac{\partial k}{\partial r_l}\right), \; v = \frac{\sqrt{2}r_l^3}{2}. \tag{3}$$

If knowing the interaction potential φ Eq. (3) allows us to determine the nearest neighbor distance r_{1X} (P, 0) (X = A, A_1, A_2, B) at pressure P and 0K. If knowing r_{1X} (P, 0) we can determine the parameters k_X (P, 0), γ_{1X} (P, 0), γ_{2X} (P, 0), γ_X (P, 0) at pressure P and 0K for each case of atom X. Then, the displacement y_{0X} (P, T) of atom X from equilibrium position at temperature T and pressure P is calculated as in [20]. From that, we can caculate the nearest neighbor distance r_{1X} (P, T) at temperature T and pressure P as follows

$$r_{1B}(P, T) = r_{1B}(P, 0) + y_{A_1}(P, T),\; r_{1A}(P, T) = r_{1A}(P, 0) + y_A(P, T),$$
$$r_{1A_1}(P,T) \approx r_{1B}(P,T), r_{1A_2}(P,T) = r_{1A_2}(P,0) + y_{A_2}(P,T). \tag{4}$$

The mean nearest neighbor distance between two atoms A in FCC interstitial alloy AB at temperature T and pressure P has the form [9, 16]

$$\begin{gathered}\overline{r_{1A}(P,T)} = \overline{r_{1A}(P,0)} + \overline{y(P,T)},\\ \overline{r_{1A}(P,0)} = (1-c_B)\,r_{1A}(P,0) + c_B r'_{1A}(P,0), r'_{1A}(P,0) = \sqrt{2}\,r_{1B}(P,0),\\ \overline{y(P,T)} = (1-15c_B)\,y_A(P,T) + c_B y_B(P,T) + 6c_B y_{A_1}(P,T) + 8c_B y_{A_2}(P,T).\end{gathered} \tag{5}$$

The Helmholtz free energy of FCC interstitial alloy AB with the condition $c_A << c_B$ is determined by [9, 16]

$$\begin{gathered}\psi_{AB} = (1-15c_B)\psi_A + c_B\psi_B + 6c_B\psi_{A_1} + 8c_B\psi_{A_2} - TS_c,\\ \psi_X \approx U_{0X} + \psi_{0X} + 3N\left\{\frac{\theta^2}{(k_X)^2}\left[\gamma_{2X}(Y_X)^2 - \frac{2\gamma_{1X}}{3}\left(1+\frac{Y_X}{2}\right)\right] + \right.\\ \left. + \frac{2\theta^3}{(k_X)^4}\left[\frac{4}{3}\gamma_{2X}Y_X\left(1+\frac{Y_X}{2}\right) - 2\left[(\gamma_{1X})^2 + 2\gamma_{1X}\gamma_{2X}\right]\left(1+\frac{Y_X}{2}\right)(1+Y_X)\right]\right\},\\ \psi_{0X} = 3N\theta\left[x_X + \ln\left(1-e^{-2x_X}\right)\right], Y_X \equiv x_X \coth x_X,\end{gathered} \tag{6}$$

where ψ_X is the Helmholtz free energy of one atom X, U_{0X} is the cohesive energy and S_c the configurational entropy of alloy AB.

From the equation of state, we can determine the nearest neighbor distance between two atoms $r_{1X}(P,0)(X = B, A, A_1, A_2)$ in alloy before deformation. After deformation, this distance becomes

$$r^F_{1X}(P,0) = r_{1X}(P,0)(1+\varepsilon), \quad r^F_{1X}(P,T) = r_{1X}(P,T) + \varepsilon . r_{1X}(P,0)(2+\varepsilon). \tag{7}$$

The Helmholtz free energy of FCC interstitial alloy AB after deformation ψ^F_{AB} has the same form (6) as one before deformation.

In the nonlinear deformation, the relationship between the stress and the deformation is decribed by

$$\sigma_{1AB} = \sigma_{0AB}\frac{(\varepsilon^F)^{\alpha_{AB}}}{1+\varepsilon^F}, \tag{8}$$

where σ_{0AB} and α_{AB} are constants for every interstitial alloy.

The density of deformation energy can be written in the form

$$
\begin{aligned}
f_{AB}(\varepsilon) = \frac{1}{N}(1-15c_B)\Bigg\{\Psi_A\left(\frac{1}{v_{AB}^F}-\frac{1}{v_{AB}}\right)+\frac{2\varepsilon r_{01A}^F}{v_{AB}^F}\left(\frac{\partial\Psi_A^F}{\partial r_{1A}^F}\right)_T + \\
+\frac{\varepsilon^2}{2v_{AB}^F}\left[\left(\frac{\partial^2\Psi_A^F}{\partial r_{1A}^{F2}}\right)_T\left(2r_{01A}^F\right)^2+\left(\frac{\partial\Psi_A^F}{\partial r_{1A}^F}\right)_T 2r_{01A}\right]\Bigg\}+\frac{c_B}{N}\Bigg\{\Psi_B\left(\frac{1}{v_{AB}^F}-\frac{1}{v_{AB}}\right)+ \\
+\frac{2\varepsilon r_{01B}^F}{v_{AB}^F}\left(\frac{\partial\Psi_B^F}{\partial r_{1B}^F}\right)_T+\frac{\varepsilon^2}{2v_{AB}^F}\left[\left(\frac{\partial^2\Psi_B^F}{\partial r_{1B}^{F2}}\right)_T\left(2r_{01B}^F\right)^2+\left(\frac{\partial\Psi_B^F}{\partial r_{1B}^F}\right)_T 2r_{01B}\right]\Bigg\}+ \\
+\frac{6c_B}{N}\Bigg\{\Psi_{A_1}\left(\frac{1}{v_{AB}^F}-\frac{1}{v_{AB}}\right)+\frac{2\varepsilon r_{01A_1}^F}{v_{AB}^F}\left(\frac{\partial\Psi_{A_1}^F}{\partial r_{1A_1}^F}\right)_T + \\
+\frac{\varepsilon^2}{2v_{AB}^F}\left[\left(\frac{\partial^2\Psi_{A_1}^F}{\partial r_{1A_1}^{F2}}\right)_T\left(2r_{01A_1}^F\right)^2+\left(\frac{\partial\Psi_{A_1}^F}{\partial r_{1A_1}^F}\right)_T 2r_{01A_1}\right]\Bigg\}+\frac{8c_B}{N}\Bigg\{\Psi_{A_2}\left(\frac{1}{v_{AB}^F}-\frac{1}{v_{AB}}\right)+ \\
+\frac{2\varepsilon r_{01A_2}^F}{v_{AB}^F}\left(\frac{\partial\Psi_{A_2}^F}{\partial r_{1A_2}^F}\right)_T+\frac{\varepsilon^2}{2v_{AB}^F}\left[\left(\frac{\partial^2\Psi_{A_2}^F}{\partial r_{1A_2}^{F2}}\right)_T\left(2r_{01A_2}^F\right)^2+\left(\frac{\partial\Psi_{A_2}^F}{\partial r_{1A_2}^F}\right)_T 2r_{01A_2}\right]\Bigg\}.
\end{aligned}
\tag{9}
$$

From the graph of the function $f_{AB}(\varepsilon)$ we can find the value of f_{ABmax} corresponding to the deformation ε_{AB}^F. When the deformation rate is constant, the density of deformation energy of alloy is determind by:

$$f_{AB}(\varepsilon) = C_{AB}.\sigma_{AB}.\varepsilon, \tag{10}$$

where C_{AB} is the proportional factor. At the maximum value of the density of deformation energy, we have:

$$f_{AB}\left(\varepsilon_{AB}^F\right) = f_{ABmax} = C_{AB}\sigma_{ABmax}\varepsilon_{AB}^F. \tag{11}$$

Therefore, the maximum value of stress σ_{ABmax} and the maximum real stress σ_{1ABmax} are

$$\sigma_{ABmax} = \frac{f_{ABmax}}{C_{AB}\varepsilon_{AB}^F},\ \sigma_{1ABmax} = \frac{\sigma_{ABmax}}{1+\varepsilon_{AB}^F} = \frac{f_{ABmax}}{C_{AB}\varepsilon_{AB}^F(1+\varepsilon_{AB}^F)}. \tag{12}$$

From the maximum condition of stress $\left(\frac{\partial\sigma_{ABl}}{\partial\varepsilon}\right)_{\varepsilon_{AB}^F} = 0,$ we determine the deformation ε_{AB}^F corresponding to the maximum value of real stress as follows:

$$\varepsilon_{AB}^{F}=\frac{\alpha_{AB}}{1-\alpha_{AB}},\quad \sigma_{lABmax}=\sigma_{0AB}\frac{\left(\varepsilon_{AB}^{F}\right)^{\alpha_{AB}}}{1+\varepsilon_{AB}^{F}}. \tag{13}$$

The proportional factor C_{AB} is determined from the experimental condition of stress $\sigma_{0.2AB}$ in alloy in the form:

$$C_{AB}=\frac{f_{AB}(\varepsilon_{0.2AB})}{\sigma_{0.2AB}\varepsilon_{0.2AB}}. \tag{14}$$

Then after having the value of ε_{AB}^{F} we can calculate σ_{0AB} and α_{AB}. The limit of elastic deformation of interstitial alloy AB is determined by

$$\sigma_{ABe}=E_{AB}\varepsilon_{AB}^{e}=\sigma_{0AB}\frac{\left(\varepsilon_{AB}^{e}\right)^{\alpha_{AB}}}{1+\varepsilon_{AB}^{e}}. \tag{15}$$

Here, ε_{AB}^{e} is the elastic deformation of alloy AB and E_{AB} is the Young modulus of alloy AB.

3. NUMERICAL RESULTS AND DISCUSSION

To describe the interaction between atoms Au and Si, we apply the Mie-Lennard-Jones pair interaction potential in the form [21]:

$$\phi(r)=\frac{D}{n-m}\left[m\left(\frac{r_0}{r}\right)^{n}-n\left(\frac{r_0}{r}\right)^{m}\right], \tag{16}$$

where D is the depth of potential well corresponding to the equilibrium distance r_0, m and n are determined empirically. Then, the potential parameters for the interaction Au-Si are determined by [22]:

$$D_{Au-Si}=\sqrt{D_{Au-Au}D_{Si-Si}},\ r_{0Au-Si}=\frac{1}{2}\left(r_{0Au-Au}+r_{0Si-Si}\right). \tag{17}$$

We find $m_{Au\text{-}Si}$ and $n_{Au\text{-}Si}$ by fitting the theoretical result with the experimental data for the Young modulus of interstitial alloy $AuSi_{3\%}$ at room temperature. The

Mie-Lennard-Jones potential parameters for the interactions Au-Au, Si-Si and Au-Si are given in Table 1.

Table 1

The Mie-Lennard-Jones potential parameters for the interactions Au-Au, Si-Si and Au-Si

Interaction	D [eV]	r_0 [10^{-10} m]	m	n
Au-Au [21]	0.6392	2.8751	15.56	1.96
Si-Si [23]	5.5400	2.3510	6.00	12.00
Au-Si (proposal)	1.8818	2.6131	1.25	9.94

Figure 1 and Table 2 show the dependence of the density of deformation energy $f(\varepsilon)$ and the maximum value of real stress on the deformation ε for clean metal Au. The graph $f(\varepsilon)$ has one maximum point (ε^F, f_{max}). When the temperature increases, both ε^F and f_{max} decreases. For example, at T = 500 K, we have ε^F = 7.3% corresponding to f_{max} = 9.1 GPa and at T = 700 K we have ε^F = 5.9% corresponding to f_{max} = 8.59 GPa. Knowing ε^F and f_{max}, we can determine the maximum value of real stress σ_{1max} when happens the nonlinear deformation. Note that in our calculation steps, we propose that $\sigma_{0.2}$ changes slowly with respect to temperature and concentration of interstitial atoms, *i.e.* $\sigma_{0.2}(c_{Si}, T) \approx \sigma_{0.2}(c_{Si}, 300\ K)$. That is one of causes leading to deviations between the SMM calculations and experiments. If we have the experimental data of $\sigma_{0.2}$ in different conditions, certainly our numerical calculations will have lower errors.

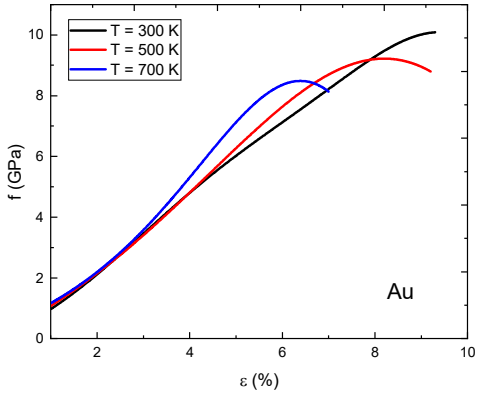

Fig. 1 – f(ε) for alloy Au at P = 0 calculated by SMM.

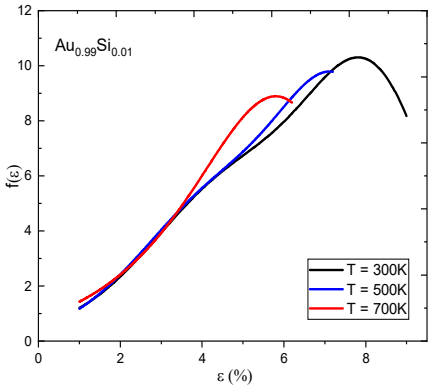

Fig. 2 – f(ε) for alloy $Au_{0.99}Si_{0.01}$ at P = 0 calculated by SMM.

Table 2

The dependence of the density of deformation energy f(ε) and the maximum value of real stress σ_{1max} on strain for Au at T = 300 K calculated by SMM

Strain ε	**0.01**	**0.02**	**0.03**	**0.04**	**0.05**	**0.06**	**0.07**	**0.08**
f(ε) (GPa)	0.95	2.16	3.46	4.77	6.02	7.17	8.22	9.20
$\sigma_{1\,max}$ (MPa)	121	135	143	147	147	144	140	136
Strain ε	0.09	0.091	0.092	0.093				
f(ε) (GPa)	10.11	10.14	10.11	9.92				
σ_{1max} (MPa)	132	131	129	125				

Table 3 and Table 4 compare the SMM results and the experimental data for the maximum value of real stress σ_{1max} [GPa] and the limit of elastic deformation σ_e [GPa] for Au at P = 0 and different temperatures.

Table 3

The value of $\varepsilon^F(f(\varepsilon^F) = f_{max})$ and the maximum value of real stress σ_{1max} (MPa) for Au at P = 0 and T = 300, 500 and 700 K calculated by SMM and from experiments

T = 300 K				**T = 500 K**		**T = 700 K**	
SMM		**EXPT[3]**	**EXPT[24]**	ε^F	$\sigma_{1\,max}$	ε^F	$\sigma_{1\,max}$
ε^F	$\sigma_{1\,max}$						
0.091	131	98÷173	100	0.073	149.73	0.06	171.79

Table 4

The elastic deformation ε^e and the limit of elastic deformation σ_e (MPa) for Au at P = 0 and T = 300 K calculated by SMM and from experiments

T = 300 K			**T = 500 K**		**T = 700 K**	
SMM		**EXPT [26,27]**	**SMM**		**SMM**	
ε^e	σ_e		ε^e	σ_e	ε^e	σ_e
0.11	99	120; 45 ÷ 300	0.17	124	0.24	152

(The Young modulus E_{Au} = 86.7 GPa by the SMM, E_{Au} = 89.1 GPa from EXPT [25])

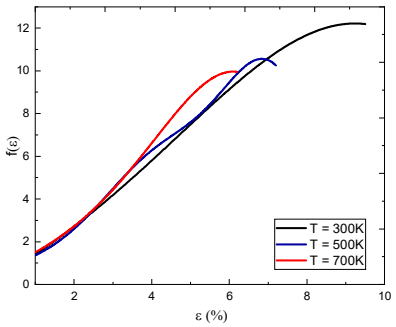

Fig. 3 – f(ε) for alloy $AuSi_{2\%}$ at P = 0 calculated by SMM.

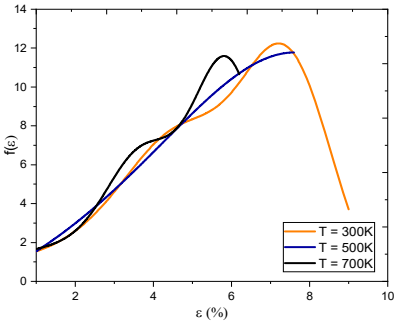

Fig. 4 – f(ε) for alloy $AuSi_{3\%}$ at P = 0 calculated by SMM.

Table 5

The limit of elastic deformation σ_e(MPa) and the maximum value of real stress $\sigma_{1\ max}$ (MPa) for AuSi at P = 0 and different temperatures and Si concentrations

c_{Si}	T (K)	σ_e	σ_{1max}
1%	300 K	127.86	165.08
	500 K	163.07	190.35
	700 K	194.10	215.81
2%	300 K	129.03	165.08
	500 K	164.12	190.35
	700 K	195.10	215.81
3%	300 K	163.62	193.25
	500 K	171.07	199.65
	700 K	212.60	233.16

Table 6

The dependence of the density of deformation energy f(ε) [GPa] and the real stress σ_1 [MPa] on strain ε (%) and pressure P [GPa] for $AuSi_{1\%}$ at T = 295 K

ε	P = 1		P = 3		P = 5		P = 7	
	f(ε)	σ_1	f(ε)	σ_1	f(ε)	σ_1	f(ε)	σ_1
1	1.08	136.89	1.03	130.41	0.97	123.57	0.92	116.44
2	2.44	153.06	2.39	150.04	2.34	146.62	2.28	142.88
3	3.92	162.45	3.91	161.92	3.89	160.97	3.85	159.68
4	5.42	166.77	5.46	167.96	5.48	168.73	5.50	169.17
5	6.86	167.35	6.96	169.67	7.04	171.60	7.10	173.20
6	8.21	165.29	8.36	168.27	8.49	171.00	8.61	173.25
7	9.45	161.49	9.64	164.72	9.81	167.71	9.97	170.46
8	10.59	156.91	10.79	159.86	10.99	162.86	11.19	165.74
9	11.70	152.75	11.85	154.67	12.04	157.17	12.25	159.85
9.5	12.05	148.31			12.54	154.30	12.73	156.70
9.6	11.97	145.68			12.63	153.73	12.83	156.07
9.7	11.56	139.08			12.73	153.17	12.92	155.44
9.8	9.59	114.05	12.43	147.91	12.83	152.61	13.01	154.81
9.9			9.31	109.60	12.92	152.04	13.10	154.19
10					13.01	151.44	13.19	153.57
10.75					12.77	137.35	13.30	142.99
0.11							13.68	143.46
11.125							13.54	140.27
11.25							12.58	128.68

Table 7

The limit of elastic deformation σ_e(MPa) and the maximum value of real stress σ_{1max} (MPa) for $AuSi_{1\%}$ at T = 300 K and different pressures

P (GPa)	0	1	3	5	7
σ_e	127.86	112	108.79	109.37	975.61
$\sigma_{1\ max}$	165.08	148.31	147.91	151.44	143.46

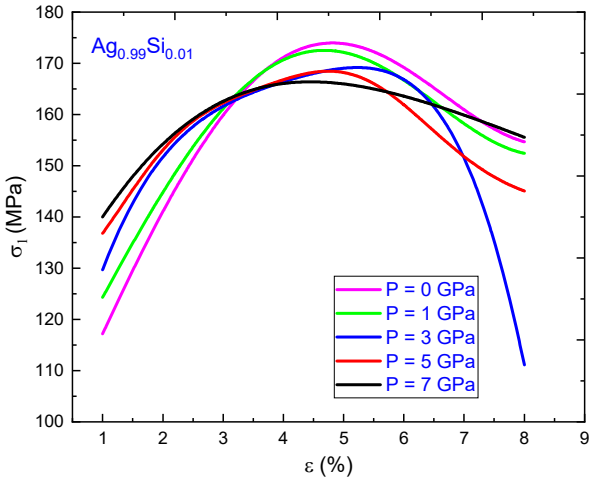

Fig. 5 – σ(ε) for alloy $AuSi_{1\%}$ at T = 300 K and different pressures calculated by SMM.

4. CONCLUSION

From the obtained theoretical results, by building the Mie-Lennard-Jones potential parameters for interactions Au-Au, Si-Si and Au-Si we calculated numerically quantities of nonlinear deformations of interstitial alloy AuSi. We obtained the stress – strain curve for metal Au and alloy AuSi. The SMM calculations of the Young modulus, the maximum value of real stress and the limit of elastic deformation are compared with experiments for Au.

Acknowledgements. This work was supported by the National Foundation for Science and Technology Development (NAFOSTED) of Vietnam under Grant No.103.02-2017.316.

REFERENCES

1. K. E. Mironov, *Interstitial alloy*, Plenum Press, New York, 1967.
2. A. Smirnov, *Theory of Interstitial Alloys*, Nauka, Moscow, 1979.
3. L. V. Tikhonov and G. I. Kononenko, *Mechanical properties of metals and alloys*, Kiev, 1986.
4. P. A. Korzhavyi, I. A. Abrikosov, B. Johansson, A. V. Ruban and H. L. Skriver, Phys. Rev. B **59**, 11693 (1999).
5. T. T. Lau, C. J. Först, X. Lin, J. G. Gale, S. Yip and K. J. Van Vliet, Phys. Rev. Lett. **98**, 215501 (2007).
6. M. Li, Phys. Rev. B **62**, 13979 (2000).
7. K. Masuda – Jindo, V. V. Hung and P. D. Tam, Calphad **26**, 1, 15 (2002).
8. J. K. Baria, Czechoslavak J. Phys, **54**, 4, 469 (2004).
9. N. Q. Hoc, B. D. Tinh, L. D. Tuan and N.D. Hien, Journal of Science of HNUE, Mathematical and Physical Sciences **61**(7), 47–57 (2016).
10. N. Q. Hoc and N. D. Hien, *Proc. of the 10th National Conference on Solid State Physics and Material Science (SPMS)*, Hue City, 19–21 October, 911–914 (2017).

11. N. Q. Hoc, N. T. Hoa and N. D. Hien, *Scientific Journal of Hanoi Metropolitan University, Natural Science and Technology* **20**, 55–66 (2017).
12. N. Q. Hoc and N. D. Hien, HNUE Journal of Science, Natural Sciences **63** (3), 23–33 (2018).
13. N. Q. Hoc and N. D. Hien, 42nd Vietnam National Conference on Theoretical Physics, *IOP Conf. Series: Journal of Physics: Conf. Series* 1034 (2018) 012005, DOI: 10.1088/1742-6596/1034/1/012005.
14. N. Q. Hoc, B. D. Tinh and N. D. Hien, *High Temperature Materials and Processes* **38**, 264–272 (2018). https://doi.org/10.1515/htmp-2018-0027.
15. N. Q. Hoc, N. T. Hoa, N. D. Hien and D. Q. Thang, *HNUE Journal of Science, Natural Sciences* **63** (6), 57–65 (2018).
16. N. Q. Hoc, N. D. Hien and D. Q. Thang, *HNUE Journal of Science, Natural Sciences* **63** (6), 74–83 (2018).
17. B. D. Tinh, N. Q. Hoc, D. Q. Vinh, T. D. Cuong and N. D. Hien, *Advances in Materials Science and Engineering*, **2018**, 5251741 (2018), https:// doi.org/10.1155/2018/5251741.
18. N. Q. Hoc, T. D. Cuong and N. D. Hien, Proc. the ACCMS-Theme Meeting on *Multiscale Modelling of Materials for Sustainable Development*, 7th–9th September, 2018, VNU, Hanoi, Vietnam, VNU Journal of Sciences: Mathematics-Physics **35** (1), 1–12 (2019).
19. N. Q. Hoc, N. T. Hoa and N. D. Hien, HNUE Journal of Science, Natural Sciences **64** (6), 45–56 (2019).
20. N. Tang and V. V. Hung, Physica status solidi (b) 149, 511 (1989); 161, 165 (1990); 162, 371 (1990); 162, 379 (1990).
21. M. N. Magomedov, High Temperature **44** (4), 513–529 (2006).
22. R. J. Good and C. J. Hope, The Journal of Chemical Physics **53** (2), 540–543 (1970).
23. M. N. Magomedov, Russian Microelectronics **40** (8), 567–573 (2011).
24. https://en.wikipedia.org/wiki/Ultimate_tensile_strength. [Accessed April 05, 2020]
25. D. R. Lide, *CRC Handbook of Chemistry and Physics*, 86th ed., Taylor & Francis, Boca Raton London, New York, Singapore, 2005.
26. https://en.wikipedia.org/wiki/Gold. [Accessed April 04, 2020]
27. https://www.azom.com/properties.aspx?ArticleID=600. [Accessed April 04, 2020]